1.5.5.3.3.2 Antiferromagnetism

X_2YZ X = 4d, Y = 3d

X = 8A: Pd, Ru
Y = 7A: Mn; 8A: Fe
Z = 3B: In; 4B: Si, Ge; 5B: Sb

Pd_2MnIn

This is the prototype Heusler antiferromagnet which has been extensively studied since the effects of B2 atomic disorder significantly changes the magnetic properties [88W1]. In the ordered $L2_1$ structure Pd_2MnIn has a Néel temperature of 140 K and type 2 antiferromagnetic order, in which the propagation vector is along the [111]. The atomic disordering temperature of the compound is 880 K and if quenched, produces complete B2 disorder. For this compound the Néel temperature has been suppressed to ≈ 80 K. In the B2 structure, the Mn atoms occupy a simple cubic environment and the magnetic structure is consistent with a type-G arrangement. However, magnetisation measurements in fields up to 5 T have revealed a magnetic phase transition at ≈ 8 K in a polycrystalline sample ordered in the $L2_1$ structure.

Three new antiferromagnetic Heusler alloys based on Ru have been reported. The Néel temperatures of Ru_2MnGa and Ru_2MnSb are 200 K and 295 K, respectively. Above the Néel temperature the susceptibilities obey a Curie-Weiss law yielding Θ = 95.5 K and p_{eff} = 4.9 μ_B for Ru_2MnSb and Θ = – 46.6 K and p_{eff} = 4.1 μ_B for Ru_2MnGe. The deviation in the susceptibility of Ru_2MnSb around 100 K is due to a realignment of the spins in the ordered state.

In the case of Ru_2FeSi a Néel temperature of 200 K has been reported.

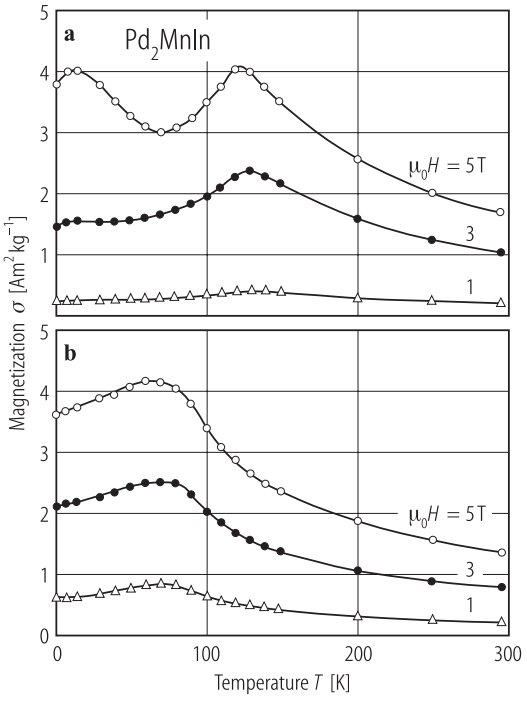

Fig. 115. (a) Magnetisation of an atomically ordered $L2_1$ sample of Pd_2MnIn (annealed at 500 °C); (**b**) An atomically disordered B sample of Pd_2MnIn (quenched from 800 °C) for different applied fields ranging from 1 to 5 T [95D1].

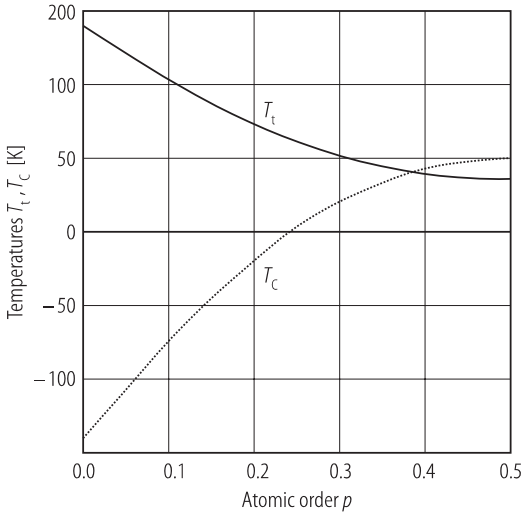

Fig. 116. Calculated AF2 transition temperature T_t(full line) and Curie temperature T_C (dotted line) as a function of atomic order p [95D1].

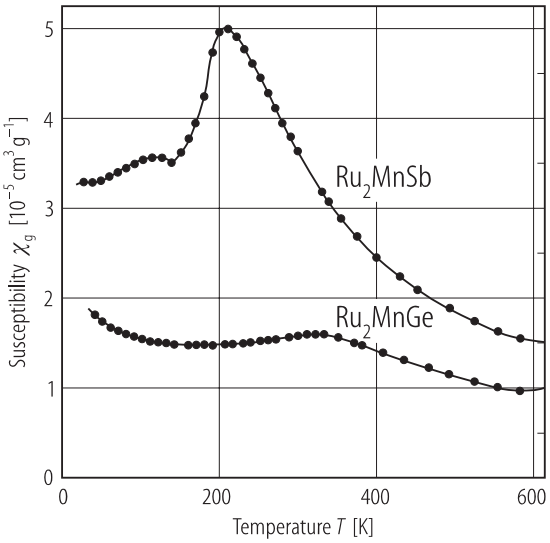

Fig. 117. Temperature dependence of the magnetic susceptibility of Ru_2MnSb and Ru_2MnGe [95G1].

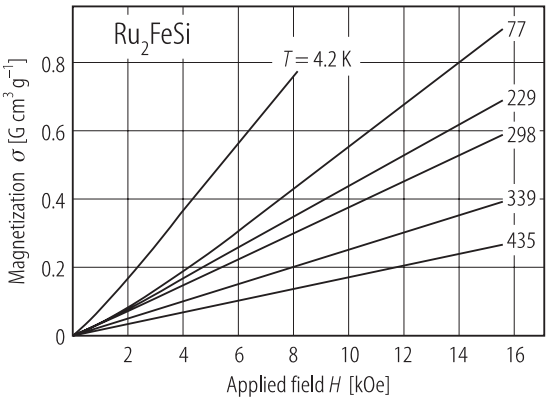

Fig. 118. Magnetic isothermals of Ru_2FeSi plotted in the form of magnetisation vs. applied magnetic field [85M3].

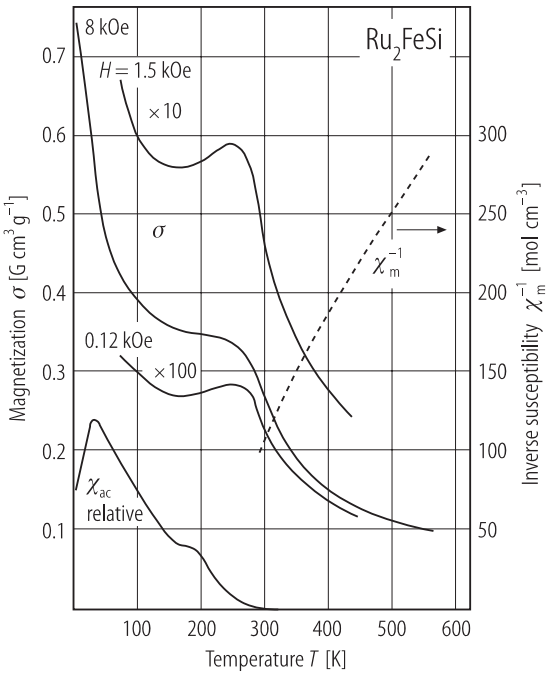

Fig. 119. The thermal variation of the magnetisation of Ru_2FeSi for several applied fields. Also shown in the figure is the temperature dependence of the ac susceptibility and the static reciprocal susceptibility [85M3].

X_2YX X = 4d, Y = 3d

X = 8A: Ir
Y = 7A: Mn
Z = 3B: Ga

The magnetic properties of Ir_2MnGa are very similar to the related $C1_b$ compound IrMnGa. The susceptibility shows a maximum around 65 K and Curie-Weiss behaviour above 100 K with an effective moment of 4.01μ_B/Mn and Θ = – 62 K.

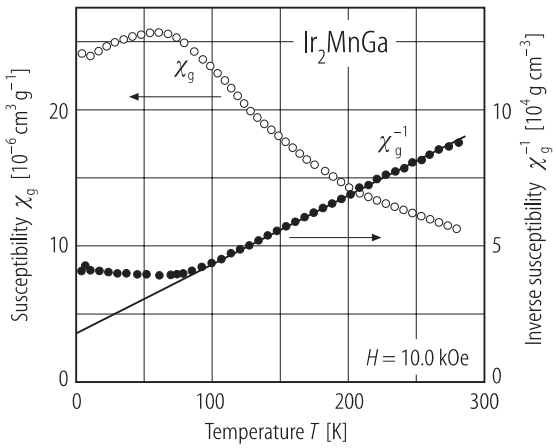

Fig. 120. Temperature dependence of the susceptibility and reciprocal susceptibility of Ir_2MnGa. (T_n = 65 K, Θ = 62 K, p_{eff} = 4.01 μ_B/Mn, a = 6.05 Å) [88Y1].

1.5.5.3.3.3 Paramagnetic

X_2YZ X = 4d, Y = 3d

X = 8A: Pd
Y = 4A: Ti
Z = 3B: Al, Ga, In; 4B: Sn

Pd_2TiZ

These compounds, which have been classified as superweak magnetic, are characterised by small moments and high characteristic temperatures. The bulk susceptibility measurements on Pd_2TiIn suggest antiferromagnetism below ≈ 110 K, but neutron diffraction measurements reveal a structural phase transition at 110 K. Above this temperature the susceptibility is Curie-Weiss, yielding p_{eff} = 4.9 μ_B and Θ = 33.4 K, values surprisingly close to those of Pd_2MnIn. The other compounds in the series have a distinct hysteresis in the magnetisation process.

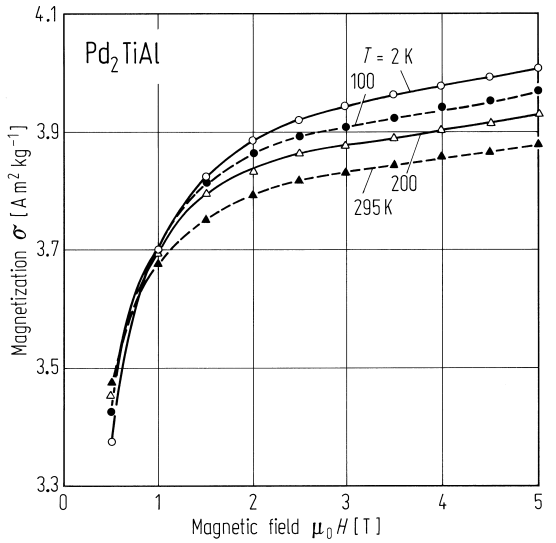

Fig. 121. Isotherms of magnetisation vs. applied field for Pd_2TiAl [94N1].

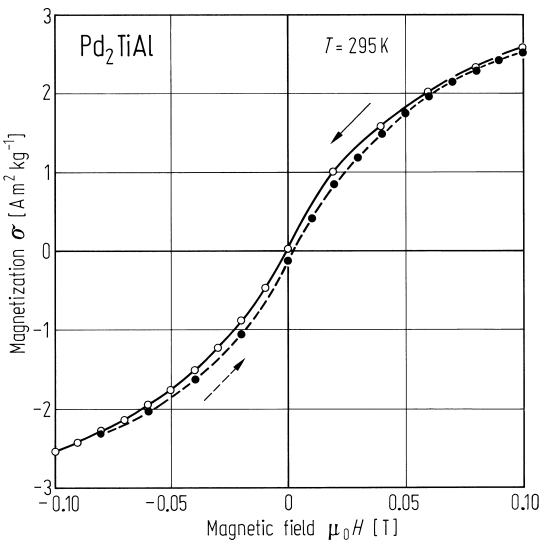

Fig. 122. Magnetic hysteresis of Pd_2TiAl measured at 295 K [94N1].